Elementary Phase Diagrams: Principles and Methods[§]

James A. D. Connolly, ERDW-ETH Zurich CH-8092

"Phase diagrams are the beginning of wisdom..." – Sir William Hume-Rothery (1899-1969).

Chemical thermodynamics owes its origin to Gibbs' treatment of thermodynamic surfaces, but this way of thinking about thermodynamics is often neglected in teaching. This method is particularly useful for understanding phase equilibria involving phases of variable composition (solutions, melts, etc.). The first section of these notes reviews several familiar thermodynamic concepts in the context of Gibbs energy surfaces (i.e., $\overline{G} - X$ diagrams). The following section discusses the basic types of phase diagrams and the notes conclude with a short, incomplete, review of some of the methods currently used to compute petrologic phase equilibria.

G–X Diagrams

"Thermodynamics is the science of the impossible. It enables you to tell with certainty what cannot happen. Thermodynamics is noncommittal about the things that are possible. Thermodynamics is at its best when nothing can happen, a condition called equilibrium. The concept of equilibrium has been fruitfully extended to reversible processes. Here everything is impossible except one very specific process and even this process is on the verge of being impossible." – An anonymous, slightly inaccurate, wit.

The basis of equilibrium thermodynamics is the Gibbs stability criterion that states that an isobaric-isothermal-isochemical system is in stable equilibrium when its Gibbs energy (G) is a minimum. Mathematically this criterion is written

$$dG_{T,P,n} > 0, \tag{1.1}$$

an expression that implies that for a system in stable equilibrium any variation will lead to an increase in the Gibbs energy. To understand this criterion, consider a two-component phase of variable composition, i.e., a solution. If the molar Gibbs energy is plotted (the Gibbs energy of the phase per mole of components, $\overline{G}$, defined explicitly below) vs. composition (X), then a curve such as that shown by the heavy curve in Fig 1.1a will be obtained. This curve defines the possible material states of the system. However, the system may consist of any number of parts, each of which will be described by a point on the $\overline{G} - X$ curve of the phase. The only

[§] These notes were published in "Pressure and Temperature Evolution of Orogenic Belts," Lectures of the V Summer School, Geologia e Petrologia dei Basamenti cristallini of the University of Siena and the Italian National Research Council, 1992, p 203-220.

constraints on the system and its parts are that the mean (mole weighted) composition and Gibbs energy of the parts must be equal, respectively, to the bulk composition and Gibbs energy of the system. Suppose then that the system has a bulk composition X^{system} and consists of two equal parts **a** and **b**, the Gibbs energy of the system will be given by the point on the line connecting the $\overline{G} - X$ coordinates of **a** and **b** at X^{system} ($\overline{G}^{\textbf{system}}$ in Fig 1.1). Now, considering the Gibbs' stability criterion, it is clear that this is not the lowest Gibbs energy for the system, for example if we change the composition of the parts to **a'** and **b'**, we can lower the Gibbs energy of the system. In fact, we can keep lowering the Gibbs energy of the system by making the composition of the two parts of the system approach the bulk composition of the system X^{system}, and the minimum Gibbs energy will be attained when both parts are of composition X^{system}. In other words, the system will only be in stable equilibrium if the phase has the same composition in all parts of the system. It is noteworthy that this would be true for any bulk composition of the system because the $\overline{G} - X$ surface* of the phase is concave with respect to the $\overline{G}$ ordinate. Solutions that have this property are known as continuous solutions, olivine (forsterite-fayalite) and most Mg-Fe mineral solutions are examples of continuous solutions.

There is no reason to expect that the $\overline{G} - X$ surface of all phases should be concave, indeed they are not; however, for regions of composition in which the $\overline{G} - X$ surface of a phase is convex the phase (with the corresponding composition) is always unstable. This is illustrated in Fig 1.1b, consider that a system consists initially of a homogeneous phase **a**, the system can lower its Gibbs energy if the phase unmixes into two parts with compositions on either side of **a**, and it will minimize its Gibbs energy if the parts have the compositions **a'** and **b'**. This would be true for any bulk composition between **a'** and **b'**. Such solutions are said to exhibit immiscibility, and the compositions **a'** and **b'** locate the limbs of the solutions solvus at constant *P* and *T*, Orthoclase (orthoclase-albite) and Muscovite (muscovite-paragonite) are mineral solutions with immiscibility (at least at low temperature). It is also conceivable that the $\overline{G} - X$ surface of a solution is always convex as in Fig 1.1c. In this case, a mechanical mixture of the solution end-members is always more stable than any solution composition, and so, for practical purposes, there is no solution. In principle the $\overline{G} - X$ surface of any solution cannot be always convex, that is, on a fine enough scale, the surface must be concave

* Throughout these notes the terms surface and plane are used in a general geometric sense, i.e., in an *n*-dimensional space these are *n*-dimensional nonlinear and linear geometric elements. Thus, in the context of a 2-dimensional (c=2) $\overline{G} - X$ diagram, a curve is a surface and a line is a plane.

near the end-member compositions (e.g., there is some solubility of Zr in forsterite, and likewise some solubility of Mg in Zircon). In the limit that these concave regions are small they can be ignored and the end-members regarded as phases with fixed compositions, i.e. compounds (e.g. zircon and forsterite, or α and β in Fig 1.1c). The $\overline{G} - X$ surface of a compound is actually a point rather than a surface.

In general the shape of $\overline{G} - X$ surfaces varies as a function of both *P* and *T*; thus, a solution maybe continuous at one $P - T$ condition and immiscible at another.

The Gibbs Energy

The Gibbs energy of a *c*-component system or phase is defined by the summation

$$G = \sum_{i=1}^{c} n_i \mu_i \tag{1.2}$$

where n_i is the number of moles of component *i*, and μ_i is the chemical potential of the component defined as

$$\mu_i \equiv \left(\frac{\partial G}{\partial n_i} \right)_{P,T,(n_j, j \neq i)} \tag{1.3}$$

The significance of μ_i is that it tells us how the Gibbs energy will change if we change n_i by an infinitesimal amount, holding all the other independently variable properties (P, T, $n_{j,j \neq i}$) of the system or phase constant. The physical importance of chemical potentials will be considered in the next section.

Eq (1.2) enables us to calculate *G* for a system of arbitrary size, as defined by the number of moles of each component, but in the study of phase relations we are only concerned with the state of the system, which is determined by its pressure, temperature, and composition. Thus it is convenient to define a property that gives the *G* as a function of composition, this property is known as the molar Gibbs energy and is related to *G* by:

$$\overline{G} = \frac{G}{\sum_{i=1}^{c} n_i} \tag{1.4}$$

If the composition (or "mole fraction") of component *i* is defined as:

$$X_j = \frac{n_j}{\sum_{i=1}^{c} n_i} \tag{1.5}$$

then by substituting Eq (1.2) into Eq (1.4) we obtain:

$$\overline{G} = \sum_{i=1}^{c} X_i \mu_i \tag{1.6}$$

Any expression in terms of the integral properties (G and $n_1 \ldots n_c$) is equally valid in terms of ($\overline{G}$ and $X_1 \ldots X_c$), but the advantage of the second form is that it involves one less independent variable because of the constraint:

$$\sum_{i=1}^{c} X_i = 1 \tag{1.7}$$

Thus Eq (1.2) is a linear equation in c-dimensional space, whereas Eq (1.6) is a linear equation in $c-1$-dimensional space.

If you are familiar with thermodynamics, you may be thinking that there is something missing from Eqs (1.2) and (1.6), namely P and T, in which case you are confusing the differential form of the Gibbs energy:

$$\mathbf{d}G = -S\mathbf{d}T + V\mathbf{d}P + \sum_{i=1}^{c} \mu_i \mathbf{d}n_i \,, \tag{1.8}$$

with the integrated forms given here, in which the P, T dependence of G or $\overline{G}$ is hidden in the chemical potentials. Eq (1.8) is the basis for calculating the change in G from one condition to another through the use of complicated sounding things like heat capacity, isobaric expansivity, isothermal compressibility, Margules expansions, and enthalpy. Although such calculations can be arithmetically complex, they are unimportant for understanding thermodynamics, and can be summarized by the simple statement:

$G = \mathrm{f}(P, T, n_1 \ldots n_c)$. (1.9)

In practice, it is rarely even necessary to know the actual form of this function, one simply looks up the value at the P, T, and $n_1 \ldots n_c$ of interest, or calculates them with a computer program such as the Perple_X program FRENDLY. There is a trick though, the values one looks up, or calculates, are the Gibbs energy per molar formula unit of the phase in question. A molar formula unit contains ν_i moles of component i (i=1 ... c), therefore from Eq 1.4:

$$\overline{G} = \frac{G^{\mathbf{m}}}{\sum_{i=1}^{c} \nu_i} \tag{1.10}$$

Suppose we have calculated G of enstatite ($MgSiO_3$). If we are interested in a system with the components MgO and SiO_2, then $\nu^{\mathbf{en}}_{\mathbf{MgO}} = 1$, $\nu^{\mathbf{en}}_{\mathbf{SiO2}} = 1$ $\nu_{\mathrm{en,MgO}} = 1$, and $\overline{G}_{\mathbf{en}} = G_{\mathbf{en}}/2$. Note that if we choose a different set of components for our problem $\overline{G}_{\mathbf{en}}$ will also change, e.g., if we choose Mg_2SiO_4 and SiO_2 then $\overline{G}_{\mathbf{en}} = G_{\mathbf{en}}$.

Eq (1.6) has the interesting implication that if a tangent to the $\overline{G} - X$ surface of a phase is drawn, the intersection of the tangent with the $\overline{G}$ axes of a $\overline{G} - X$ diagram gives the value of the chemical potentials in the phase when its composition corresponds to the point of

tangency (Fig 1.1). That the tangent has this property can be demonstrated by expanding Eq (1.6) for a two-component (c=2) system:

$$\overline{G} = \mu_1 X_1 + \mu_2 X_2 \tag{1.11}$$

If $X_1 = 1 - X_2$ is substituted into Eq (1.11), and the result rearranged, one obtains:

$$\overline{G} = \mu_1 + X_2 (\mu_2 - \mu_1) \tag{1.12}$$

which is the equation of a line for which $\overline{G} = \mu_1$ at $X_2 = 0$ and $\overline{G} = \mu_2$ at $X_2 = 1$.

Chemical Potentials

"Having had occasion some years ago to learn the art of lip-reading I noticed yesterday when I was giving my paper that at the end of each of my sentences you said, 'Horse shit.' Evidently you had made special note of the word 'equilibria' in the title of my paper and were from time to time reminding yourself and your neighbors of the gist of the discussion. You are, however, under a misapprehension as to the derivation of the word 'equilibria'. It does not come from equus = horse and libria = things liberated or discharged, but is from quite different roots .If you will consult a chemist you will be able to learn the real significance of the word and I may add that I feel one so highly placed in geological circles as you should make it a point to acquire some familiarity with the exact significance of common terms used in collateral sciences.

Trusting that you will not resent my corrections and suggestions I am, yours sincerely," /s/ Norman L. Bowen, April 29, 1948.

To understand the physical significance of chemical potentials, it is useful to draw an analogy between chemical potentials and temperature or pressure. There are three basic kinds of thermodynamic processes, heat (entropy) transfer, mechanical work (volume transfer), and mass transfer. A system is in stable equilibrium when no thermodynamic processes are possible. Intuitively, you will probably accept that heat transfer will only occur between two parts of a system if there is a temperature difference between the parts of the system (Fig 1.2). Moreover you know from experience that the heat will be transferred from the high-T part to the low-T part. Likewise one part of the system will only do mechanical work on the other if there is a pressure difference within the system. This work is done by the high pressure part of the system compressing the low pressure part (i.e., negative volume transfer) In these cases, we can think of temperature and pressure, respectively, as the thermal and mechanical potentials for the system, and if these potentials are uniform then no thermal or mechanical processes can occur. Chemical potentials are exactly analogous, that is, they are a measure of the potential for chemical processes (mass transfer) in a system, and in the absence of a chemical potential difference no chemical process will occur. These process occur such that mass is transferred from an area where its chemical potential is high to one in which it is low.

For those familiar with mechanics, it may be useful to note that work (W) in mechanics can be defined, with some poetic license, from the differential:

$$dW_{\text{mechanical}} = F dx \tag{1.13}$$

where dx is the displacement of an object, and F is the opposing force. The only difference between mechanics and thermodynamics is that in thermodynamics we consider three kinds of work:

$$dW_{\text{mechanical}} = P d(-V)$$
$$dW_{\text{thermcal}} = T dS \tag{1.14}$$
$$dW_{\text{chemical}} = \mu dm$$

Comparison of eqs (1.13) and (1.14) suggests that P, T, and μ can be thought of as the thermodynamic forces against which mechanical, thermal, and chemical work are done. If these forces are equal in all parts of a system, then no work will be done by any part of the system.

Returning to the two part system of Fig 1.2, it is now easy to see why Gibbs' criterion works, as the chemical potentials in different parts of the system can only be the same if all parts of the system have the same composition. This will always be true for a system in which the only possible phase is a continuous solution.

Thermodynamic Activities

Up to this point we have mainly been concerned with properties of the system rather than the properties of the phases. We can always define our system in such a way that it includes just one phase, so from Eqs (1.2) and (1.3) we can express the Gibbs energy of phase k

$$G^k = \sum_{i=1}^{c} n_i \left(\frac{\partial G^k}{\partial n_i} \right)_{P,T,(n_j, j \neq i)} \tag{1.15}$$

or

$$\overline{G}^k = \sum_{i=1}^{c} X_i^k \left(\frac{\partial G^k}{\partial n_i} \right)_{P,T,(n_j, j \neq i)} \tag{1.16}$$

Although it is probably apparent that in an equilibrium system

$$\left(\frac{\partial G^k}{\partial n_i} \right)_{P,T,(n_j, j \neq i)} = \left(\frac{\partial G}{\partial n_i} \right)_{P,T,(n_j, j \neq i)} = \mu_i \tag{1.17}$$

It is often useful to distinguish phase properties from system properties by defining the partial molar free energy of a component in a solution as

$$\overline{G}_i^k \equiv \left(\frac{\partial G^k}{\partial n_i} \right)_{P,T,(n_j, j \neq i)} \tag{1.18}$$

in which case Eq (1.15) can be written for a two-component solution

$$\overline{G}^k = \sum_{i=1}^{c} X_i^k \overline{G}_i^k \ . \tag{1.19}$$

Eq (1.19) suggests that one way of thinking about the partial molar Gibbs energy of the component *i*, is to regard it as the molar Gibbs energy that the component has in the solution. In practice solutions are usually described in terms of the properties of their end-member compositions, by introducing a quantity known as the thermodynamic activity of the end-member defined as

$$a_i^k \equiv \exp\left(\frac{\overline{G}_i^k - \overline{G}_i^\circ}{\mathbf{R}T} \right) \tag{1.20}$$

where $\overline{G}_i^\circ$ is the molar Gibbs energy of the solution *k* when it has the composition of endmember *i*. The form of the expression for the activity is chosen that so, to a first approximation, it may be regarded as a measure of the concentration of the end-member in the solution, i.e., $a_i^k \approx X_i^k$; but more generally $a_i^k \approx f(P,T,X_i^k)$. In practice, Eq (1.20) is usually rearranged to

$$\overline{G}_i^k = \overline{G}_i^\circ + \mathbf{R}T \ln a_i^k \tag{1.21}$$

so that $\overline{G}_i^k$ is expressed in terms of tabulated or measurable quantities, the values of $\overline{G}_i^k$ obtained in this way can then be used, if desired, in Eq (1.19) to obtain the molar Gibbs energy of the solution. I have assumed here that the composition of the components and the solution end-members are identical, when this is not the case it is necessary to introduce stoichiometric factors, but the fundamental principles remain the same.

To obtain a physical understanding of activity it may be helpful to consider an osmotic system (Fig 1.3). Here the main portion of the system contains a two-component solution such as biotite (modeled as a solution between the Fe-endmember annite "ann" and the Mg-endmember phlogopite "phl"), which is separated from two, initially empty, chambers by rigid membranes that are permeable with respect to only one of the endmembers, i.e., osmotic membranes. Since the pressures in these chambers is independent of the pressure on the main portion of the system, we can arrive at an equilibrium condition in which the chambers are filled with pure endmembers at pressures dictated by the constraint that the partial molar Gibbs energy of the endmember must be equal in both the chamber and the main portion of the system, e.g., for the phlogopite endmember we have

$$\overline{G}_{\mathbf{phl}}^{\mathbf{Bio}}(P,T,X) = \overline{G}_{\mathbf{phl}}^\circ(P_{\mathbf{phl}},T) \tag{1.22}$$

where it is essential to realize that although $P \neq P_{\mathbf{phl}}$, the partial pressure P_{phl} is a function of the total *P* on the biotite solution through Eq (1.22). Activities are simply a means of

accounting for this difference, this can be done explicitly in terms of pressure in which case the activity is referred to as a fugacity as in

$$\bar{G}^{\mathbf{Bio}}_{\mathbf{phl}}\left(P,T,X\right)=\bar{G}^{\circ}_{\mathbf{phl}}\left(P_{\mathbf{phl}},T\right)=\bar{G}^{\circ}_{\mathbf{phl}}\left(P_{\mathbf{r}},T\right)+\mathbf{R}T\ln f_{\mathbf{phl}}$$

where P_r is an arbitrary reference pressure, and, in the limit of an ideal solution, the fugacity $f_{phl} = P_{phl}$. However, for solids it is more conventional to define the properties of the pure endmember at the total pressure, i.e.

$$\bar{G}^{\mathbf{Bio}}_{\mathbf{phl}}\left(P,T,X\right)=\bar{G}^{\circ}_{\mathbf{phl}}\left(P_{\mathbf{phl}},T\right)=\bar{G}^{\circ}_{\mathbf{phl}}\left(P,T\right)+\mathbf{R}T\ln a_{\mathbf{phl}}$$

as in Eq (1.21). It is noteworthy that such definitions are arbitrary and introduce artificial complexity into thermodynamic theory.

Heterogeneous Systems

In the previous section it has been argued that Gibbs' stability criterion requires that the chemical potentials of each component must be uniform in all parts of a stable equilibrium system. For a system composed of a single continuous solution, this implies that all parts of the system must have the same composition because the values of the chemical potentials are different for every composition. In systems where more than one phase may occur there will be a separate $\bar{G}-X$ curve corresponding to every possible phase (e.g., α, β, γ, and δ in Fig 1.4). As the chemical potentials of the components can be determined for any composition of any phase by drawing a tangent line or plane if c>2) at the composition of interest, it is evident that the chemical potentials of the components must be equal in phases which are tangent to a common line in $\bar{G}-X$ space. In general, such phases will not have the same composition, but because the chemical potentials are uniform no thermodynamic process may occur and the phases will be in equilibrium. Thus, the Gibbs stability criterion requires that in a c-component heterogeneous system composed of p coexisting phases:

$$\mu_i^1=\ldots=\mu_i^p \qquad i=1\ldots c \tag{1.23}$$

Since the chemical potential of a component in the system is identical to the partial molar Gibbs energy of the component in each phase, Eq (1.23) can also be written

$$\bar{G}_i^1=\ldots=\bar{G}_i^p \qquad i=1\ldots c \tag{1.24}$$

The foregoing discussion has been simplified in that in addition to thermal, mechanical, and chemical processes, thermodynamics has spontaneous processes (Fig 1.2) that occur (in theory) in the absence of any potential gradients (in reality, or in statistical mechanics, which is at least closer to reality, they occur because of microscopic gradients). Thus, the equality of potentials at equilibrium is considered a necessary, but not sufficient criterion for stable equilibrium, and it becomes necessary to distinguish stable, metastable, and unstable equilibria. In unstable equilibria, there are no potential gradients in the system, but the

composition of at least one phase is in a convex region of the $\overline{G} - X$ surface of the phase (e.g., point **a** in Fig 1.1b). In metastable equilibria, all the phases have compositions along the concave portions of their $\overline{G} - X$ surfaces, but there is an accessible state (involving at least one additional phase) of lower Gibbs energy (e.g., the equilibrium of phases δ and γ, tangent to the dashed line in Fig 1.4b, is metastable with respect to phases β and α).

The fundamental problem in equilibrium thermodynamics is the determination of the stable state of a system in which there is more than one phase possible. In fact, there is no simple solution to this problem and there are several journals (e.g., CALPHAD and the Bull. of Alloy Phase Diagrams) devoted to trying to find one, but it is easy to answer graphically. Consider the system illustrated in Fig 1.4a. We can determine all the possible stable phase assemblages by draping a rope under the $\overline{G} - X$ surfaces of all the phases and then pulling upwards on the ends of the rope (Fig 1.4a). When the rope is taut it will define the minimum $\overline{G}$ surface of the system, that is, it will define all possible stable states of the system (at constant P and T). Along this surface we can distinguish two different kinds of regions, linear regions in which the surface spans the surfaces of two phases and non-linear one-phase regions in which the surface overlaps the surface of a single phase. This exercise demonstrates three points:

1) Linear regions of the surface define the composition interval over which a particular two-phase assemblage is stable, and in such a region the compositions of the phases and the chemical potentials of the system are independent of the composition of the system.
2) Because the minimum $\overline{G}$ surface of the system is never convex, the chemical potential of any component must always increase if the composition of the component in the system is increased.
3) If the surfaces of the phases are independent (and they are) and the $P - T$ condition arbitrarily specified, the probability that more than two phases will ever be stable in a two-component system is zero.

These arguments can easily be made more general, for example, in a three-component system the $\overline{G} - X$ space is three-dimensional and we can expect the maximum number of phases tangent to a three-dimensional plane to be three. This is just a graphical statement of "Goldschmidt's mineralogical phase rule," $p \leq c$ (this rule is valid if the P and T are independent; however in many geologic systems processes may buffer T and/or P so that they are not independent). More importantly, it implies that in any c-component system, if c-phases are in equilibrium their composition is a uniquely determined at any P and T.

Heterogeneous Systems Composed Entirely of Compounds

Many minerals can be regarded to a good approximation as stoichiometric compounds. This approximation has the interesting consequence that all the phase regions of the system are defined by *c*-phases (Fig 1.4c) and the chemical potentials in any region can be determined by linear algebraic solution of Eqs (1.2) or (1.6).

Thermobarometry and activity-corrected equilibria

Mineral thermobarometry makes use of the thermodynamic fact that we have just deduced, namely, that in a c-component system the compositions of the phases in a c-phase equilibrium are uniquely determined at any pressure and temperature (in practice, mineral thermobarometry is applied to a subset of a rocks real components, with the supposition that the only significant variation occurs in this subsystem, e.g., the Fe-Mg subsystem is used for garnet-biotite thermometry). Because the position of the $\overline{G} - X$ surface of each phase is an independent function of pressure and temperature, if the pressure and temperature of a system is changed, the $\overline{G} - X$ surfaces of the phases will shift relative to each other and hence the compositions of coexistent phases will also change as illustrated by Fig 1.5a.

In the foregoing discussion we have been using thermodynamics to tell us what composition phases will have at a given $P - T$, mineral thermobarometry turns the problem around, that is we observe certain mineral compositions and try to find the $P - T$ at which the minerals were in equilibrium. To demonstrate how this is done consider the equilibrium of garnet and biotite in the K_2O-FeO-MgO-Al_2O_3-SIO_2-H_2O system. Without going into the gory details of thermodynamic projections, accept that under certain circumstances we can reasonably represent the equilibrium of these two minerals by the system MgO-FeO (i.e., this would be true when biotite and garnet coexist with, e.g., quartz, muscovite, kyanite and water) where each mineral forms a continuous solution between MgO and FeO end-member compositions. If garnet and biotite are in equilibrium, then from Eq (1.23) at the pressure and temperature of the equilibrium the partial molar Gibbs energy of MgO and FeO end-member compositions of both phases must be identical, i.e., $\overline{G}^{\mathbf{Gt}}_{\mathbf{almandine}} = \overline{G}^{\mathbf{Bio}}_{\mathbf{annite}}$ (or $\mu^{\mathbf{Gt}}_{\mathbf{FeO}} = \mu^{\mathbf{Bio}}_{\mathbf{FeO}}$) and $\overline{G}^{\mathbf{Gt}}_{\mathbf{pyrope}} = \overline{G}^{\mathbf{Bio}}_{\mathbf{phlogopite}}$ (or $\mu^{\mathbf{Gt}}_{\mathbf{MgO}} = \mu^{\mathbf{Bio}}_{\mathbf{MgO}}$). From Eq (1.21), these equalities can be reformulated as

$$\Delta\overline{G}_1 = 0 = \overline{G}^{\mathbf{Gt}}_{\mathbf{alm}} - \overline{G}^{\mathbf{Bio}}_{\mathbf{ann}} = \Delta\overline{G}^{\circ}_1 + \mathbf{R}T \ln K_1 \qquad (1.25)$$

where

$$\Delta\overline{G}^{\circ}_1 \equiv \overline{G}^{\circ}_{\mathbf{alm}} - \overline{G}^{\circ}_{\mathbf{ann}}$$

$$\ln K_1 \equiv \ln a^{\mathbf{Gt}}_{\mathbf{alm}} - \ln a^{\mathbf{Bio}}_{\mathbf{ann}} = \ln \frac{a^{\mathbf{Gt}}_{\mathbf{alm}}}{a^{\mathbf{Bio}}_{\mathbf{ann}}} \approx \ln \frac{X^{\mathbf{Gt}}_{\mathbf{alm}}}{X^{\mathbf{Bio}}_{\mathbf{ann}}} \qquad (1.26)$$

The condition $\Delta\bar{G}_1 = 0$ is sometimes mistakenly called a stability criterion, but in fact it is a necessary, but not sufficient, condition for the equilibrium of the garnet and biotite. Since the value of $\Delta\bar{G}_1^\circ$ is a simple function of pressure and temperature Eq (1.25) invariably defines a curve as a function of pressure and temperature for any pair of observed, or arbitrarily chosen, biotite and garnet compositions (Fig 1.5d). The condition $\Delta\bar{G}_1 = 0$ is sometimes mistakenly called a stability criterion, but in fact it is a necessary, but not sufficient, condition for the equilibrium of the garnet and biotite. Another common mistake in geological literature is the claim that condition $\Delta\bar{G}_1 = 0$ defines the activity-corrected equilibrium of the univariant reaction (after projection through various components)

alm = ann. (1.27)

This is a dangerous falsehood for two reasons: (i) the "equilibrium" curve does not define the conditions of a reaction that will be observed in any real system (except the pure FeO system); and (ii) geologists frequently assume that all of the pressure-temperature conditions defined by this "equilibrium" are the possible conditions at which an observed mineral assemblage formed. This second misconception is the root of all evil in thermobarometry, because in general the conditions of the "equilibrium" do not correspond to real equilibrium conditions. The reason for this is that we have only solved for the condition $\mu_{\mathbf{FeO}}^{\mathbf{Gt}} = \mu_{\mathbf{FeO}}^{\mathbf{Bio}}$, but we have not made use of the second condition $\mu_{\mathbf{MgO}}^{\mathbf{Gt}} = \mu_{\mathbf{MgO}}^{\mathbf{Bio}}$. Fig 1.5c-f illustrates that if we solve only one chemical potential equality for *P* or *T* (and it is always possible to find a solution to just one), it is quite probable that the second equality will not be satisfied. In other words, either the mineral compositions are not the equilibrium compositions (very probable), or the thermodynamic formulation of the thermobarometer is incorrect (even more probable). The only way to test for consistency is to solve all the chemical potential equalities; unfortunately the thermodynamic data is often not available (although this is done in a few cases, such as feldspar thermometry). In the present case, analogous with Eq (1.25), the condition $\mu_{\mathbf{MgO}}^{\mathbf{Gt}} = \mu_{\mathbf{MgO}}^{\mathbf{Bio}}$ defines the conditions of a second activity-corrected equilibrium

$$\Delta\bar{G}_2 = 0 = \bar{G}_{\mathbf{py}}^{\mathbf{Gt}} - \bar{G}_{\mathbf{phl}}^{\mathbf{Bio}} = \Delta\bar{G}_2^\circ + \mathbf{R}T \ln K_2 \quad (1.28)$$

as a function of pressure and temperature. In general, Eqs (1.25) and (1.28) will only be true simultaneously at one point and this point corresponds to the only conditions at which the two phases could have been in equilibrium. It should be evident from our "osmotic" equilibrium example, that an activity-corrected equilibrium merely defines conditions at which the partial pressures of the endmembers satisfy the constraints imposed by conditions like Eq (1.28). However, because at equilibrium these partial pressures are not independent of the total pressure it follows that the total pressure on the phases represented by an activity corrected

equilibrium can only be identical to the nominal for an activity-corrected curve at only one point. Even when such a condition exists, e.g., where the two activity-corrected curves cross in Fig 1.5c, it is still possible that the equilibrium is metastable. This danger is illustrated by the case shown in Fig 1.5c,f where biotite is metastable with respect to garnet+staurolite. Such a result would be a strong indication of some kind of problem, but a petrologist making use of only activity-corrected equilibria would have little chance of recognizing or diagnosing it. This type of problem provides a strong argument for both incorporating solution behaviour in phase diagram calculations, and using the resulting phase diagrams for thermobarometric analysis.

An observation that follows from this discussion, is that if one has the thermodynamic data to solve all the chemical potential equalities, then any almost any assemblage of minerals with variable composition provides enough information to obtain a unique solution for both *P* and *T*.

This is not intended as an indictment of mineral thermobarometry, but rather merely a warning that mineral thermobarometry does not (as applied in petrology) provide any test for the validity of the measured compositions, nor even whether or not the observed phase assemblage was stable. In contrast, phase diagram, or equilibrium, calculations have the merit of being thermodynamically consistent in that they show (or they should, when done correctly with correct data) the stability fields and equilibrium compositions of all phases in a system. In defence of thermobarometry, it must be remarked that most thermobarometers are based on careful empirical observations, and that phase diagrams calculations are based on thermodynamic databases that have a much weaker link to the stark reality posed by real data.

What is a phase diagram?

A phase diagram is a diagram that indicates the relative amount and state of every phase in a stable equilibrium system. The most basic kind of phase diagram is an isobaric-isothermal diagram that shows the phase relations of a system as a function of composition, i.e. a composition diagram (the chemographic diagrams of petrography). Such diagrams are simply the projections of the minimum $\overline{G}$ surface onto composition space as illustrated by the vertical projection of Fig 1.6. By projecting the tangents of the minimum $\overline{G}$ surface onto the $\overline{G}$ axis of a $\overline{G} - X$ diagram we can derive a second kind of phase diagram that tells us how the system would respond if we could control μ_1.

There is an interesting distinction (see Hillert 1985 for discussion) between the diagrams, in the composition diagram if we arbitrarily specify the composition of the system we have about the same probability of being in a 1-phase region as in a two-phase region. In contrast, in the μ_1 diagram we have zero probability of landing in a two-phase region (if μ_1 is arbitrarily specified, i.e., it is a true independent variable). Recognition of this difference led Korzhinskii (1959) to restate the mineralogic phase rule as $p \leq c - m$, where m is the number of independent potentials for a system.

Phase diagrams as a function of *P* and *T*

More complex phase diagrams are derived by looking at the changes in the minimum $\overline{G}$ surface as a function of variables like *P* and *T*, such phase diagrams are known as mixed-variable phase diagrams. To illustrate how mixed-variable diagrams can be computed consider a system with three phases, α, β, and γ, such that at low *T*, only α and γ are on the minimum $\overline{G}$ surface (Fig. 1.7). Then we have three phase fields, α, α+γ, and γ. Now, if the Gibbs energy of β decreases relative to the other phases as temperature increases, then eventually the system will reach a condition (T_2) at which all three (c+1) phases, α, β, and γ are simultaneously tangent to a $\overline{G} - X$ plane. This condition is a c+1-phase equilibrium, if we cross the equilibrium condition α+γ will react to form β. Any c+1-phase equilibrium can be described by a mass balance reaction, the stoichiometry of which will depend on the compositions of the phases as given by their points of tangency with the minimum $\overline{G}$ surface. When the $\overline{G} - X$ surface of β crosses the α+γ $\overline{G} - X$ plane, α+γ becomes metastable with respect to the assemblages α+β and β+γ. If temperature is increased still further, the system will reach a point ($T>T_3$) at which the $\overline{G} - X$ surface of pure β crosses that of pure α in the component 1 subsystem (i.e., at $X = 0$). This corresponds to the reaction α = β, which would never be observed in a true binary system (i.e., $0 < X < 1$), and marks the thermal limit of the assemblage α+β, a similar reaction, γ = β, will limit the stability of γ+β. You may wonder why this diagram looks so much different than the $T - X^{\mathbf{f}}_{\mathbf{CO2}}$ diagrams of petrological fame, the reason is that the X here is a composition variable of the system, whereas $X^{\mathbf{f}}_{\mathbf{CO2}}$ is the composition of a phase (that is assumed to be stable). When used as a phase diagram variable $X^{\mathbf{f}}_{\mathbf{CO2}}$ determines the potential of H_2O and CO_2 and is therefore not really a compositional variable at all, but more like a potential. For this reason, petrologists habit of calling $P - T - X^{\mathbf{f}}_{\mathbf{CO2}}$ diagrams simply $P - T - X$ diagrams is sloppy and misleading.

The foregoing procedure could be repeated for other pressures, and if the pressures were reasonably close, the resulting diagrams could be stacked upon each other, and the phase relations interpolated between the diagrams, to obtain a three-dimensional $P-T-X$ phase diagram. For simplicity, let us construct such a diagram assuming that the phase equilibria of our *T–X* diagram are only shifted to higher temperature with increasing pressure (Fig 1.8a).

P–T–X phase diagrams

Given that the phase diagram shown in Fig 1.8a is only for a binary system, and that each additional component added to the system would add another dimension to the diagram, the complexity of the phase diagram problem is apparent. In fact, multidimensional phase diagrams are in themselves to complex to be of any value and they must be simplified for our use. In this respect, there are two methods by which the phase relations of a multicomponent system may be represented in the $P-T$ plane, sectioning or projection.

P–T Phase Diagram Sections

The $P-T$ phase diagram section is conceptually simple, it is a two-dimensional slice at constant composition through the multidimensional phase diagram (Fig 1.8b). The resulting section consists of regions of $p \leq c$ phases, which represent regions of homogeneous reaction, i.e. regions where the amount and compositions of the phases vary continuously. The boundaries of such regions are distinguished from true univariant equilibria by the number of phases represented, for example in Fig 1.8b, the boundary between the β and $\beta+\alpha$ field involves only two (= *c*) phases and therefore is not a univariant equilibrium. The section in Fig 1.8b includes only phase regions of $p \leq c$ phases; however, it is possible to obtain sections that represent equilibria of $c+1$ and $c+2$ phases. For example, if a section of Fig 1.8a were constructed, at constant composition, so as to intersect the β eutectic, a $c+1$ phase equilibrium, then the section would include a line representing the eutectic reaction.

Phase diagram sections can be very useful for interpreting the phase relations of systems in which the bulk composition of the system is fixed, for example, as in isochemical metamorphism of a subducted basalt or in mantle phase relations (Saxena & Erickson 1986, Wood & Holloway 1986). There are two major disadvantages to using phase diagramsections: (i) the boundaries in sections can be extremely sensitive to the bulk composition chosen; and (ii) their application requires bulk equilibrium, however, in many crustal metamorphic rocks mineral zonation indicates that this cannot be assumed. Phase diagram sections can contain some unusual topologic features and these, as well as topologic rules for such sections are discussed in great detail by Palatnik & Landau (1963, also Hillert 1985)

P–T Phase Diagram Projections

By far the most widely used type of petrologic diagram is the $P-T$ phase diagram projection. Phase diagram projections are obtained by projecting the phase fields of a multidimensional phase diagram onto a $P-T$ coordinate frame. In principle, it is possible to project all the phase fields, however, because phase fields of fewer than c+1 phases project as overlapping fields (e.g., $\alpha+\beta$ and $\beta+\gamma$ in Fig 1.8d), as a result complete projections are so complex as to be almost meaningless. As an alternative, in the conventional Schreinemakers projection (with which you are probably familiar), only the geometric elements of the phase diagram which project as lines (univariant curves) and points (invariant points) are shown. A confusing feature of Fig 1.8d is that there are three univariant curves that limit the stability of the β. The reason this is not a violation of Schreinemakers rules is that two of the curves, $\alpha = \beta$ and $\gamma = \beta$, represent reactions which would only be observed in the pure component 1 or component 2 subsystems. In systems with more phases it is possible to get even more curves, for example consider what would happen if β had two eutectoids separated by a thermal maximum for the phase δ as in Fig 1.8e. Then we would have five univariant curves $\alpha = \beta$, $\beta = \alpha+\delta$, $\delta = \beta$, $\beta = \delta+\gamma$, and $\gamma = \beta$. In this case, each two-phase curve represents the equilibrium, and *P–T* limit of a special composition of β, such curves are known as singular curves (in systems with more components this gets even more complex). It is a general rule that if there are two c+1-phase reactions limiting the stability of a phase then there is a c-phase singular reaction limiting the stability of the phase as well. This c-phase reaction will be for a composition of the phase between the compositions of the phase in the two c+1-phase reactions. Singular reactions do not occur in systems in which there are no solutions.

As a result of projection we lose a lot of information, but the projection has the advantage of telling us the absolute $P-T$ stability field of the stable phase assemblages of the system. For example in Fig 1.8d, the curve $\alpha+\gamma = \beta$ tells us the lowest temperature that β can be stable, however, β will only appear in the system if the bulk composition of the system is between the eutectoidal compositions of α and β . Likewise from the position of the singular curves, we may deduce that the assemblages $\alpha+\beta$ and $\gamma+\beta$ will only occur at temperatures between the curve $\alpha+\gamma = \beta$ and the curves $\alpha = \beta$ the curve $\gamma = \beta$, respectively. In this example we have an unfair advantage in that we have seen the complete phase diagram, but consider what would happen if you only had the projection. In this situation, if someone were to ask you if two phases coexist, say δ and ε, you would have no way of answering from the projection alone, which only tells you there is no reaction involving δ and ε over the $P-T$ range of the projection. In essence, Schreinemakers projections tell you the changes in the topology of the

compositional phase relations for a system; thus, you must have some idea of the compositional phase relations (or better still, a composition diagram) at some $P-T$ point within the projection coordinate frame.

Computational Methods

There are two basic approaches to computing phase diagrams or projections and sections of phase diagrams, Gibbs energy minimization, and combinatorial enumeration. The following sections briefly describe each method and discuss the applications and limitations of the methods with respect to geologic problems.

Free Energy Minimization.

The oldest and most basic computational method is constrained Gibbs energy minimization, by this method the user specifies a $P-T-X$ coordinate for a system and the stable phase assemblage at this coordinate is determined. For example, the user might specify the system is at pressure P, temperature T, and composition X_1 as in Fig 1.9a. A minimization method would then determine the stable phases for these conditions and the amount and composition of each phase (i.e. phases **b** and **d**, Fig 1.9a). If this procedure were repeated for a number of different compositions at the same $P-T$ condition, the results could be used to map out the compositional phase relations of the system. This would be a 1-dimensional composition diagram; the problem with this method for calculating phase diagrams becomes apparent if we consider the effect of adding variables like P and T or additional components. For the sake of argument let us suppose that we decide to divide our X space into a grid by spacing the points so that we will have ten points along each axis (this would be rather coarse spacing). If we have a five-component system, we will have four independent composition variables and P and T, thus our grid would consist of 10^6 points. At each point we would have to do a minimization, and the number of operations for each minimization goes as πc^2, where π is the total number of possible phases. Therefore, not only would the method involve an astronomical number of operations, but also we would be left with the job of interpolating between a million grid points in six-dimensional space. The difficulty with minimization techniques is that they require as input $P-T-X$ conditions, but in a phase diagram there are an infinite number of possible $P-T-X$ conditions and there is no a priori means of choosing the important ones. Basically, using minimization methods to determine a phase diagram of more than two dimensions is like trying to map the moon with a microscope.

Although minimization methods are not practical for multidimensional phase diagrams, they have proved useful for the calculation of phase diagram sections (Fig 1.8b). For example they

have been used to calculate how the phase relations of a rock with fixed bulk composition (e.g., pyrolite) change as a function of *P* and *T* (e.g., Saxena & Eriksson 1983, Wood & Holloway 1986). More generally, minimization can be used to calculate any two-dimensional section through a multidimensional space, thus it is possible to compute how a multicomponent system behaves if only one compositional variable is changed, i.e., the pseudo-binary phase diagrams of igneous and mantle petrology fame. Minimization methods have the advantage that they are capable of treating complex solution behavior and systems with any number of components. Two recent examples of minimization programs designed specifically for geologic problems are given by DeCapitani & Brown (1987) and Harvie et al. (1987). There is also a wealth of literature on minimization techniques in the engineering and metallurgical journals (see bibliography), which has been largely ignored by the geological community.

A major drawback of minimization methods applied to crustal metamorphism problems is that the methods assume bulk equilibrium. Thus, they are not applicable to systems where mineral zonation occurs or where the phase rule is violated. An additional caveat is that the phase relations of a multicomponent system can be extremely sensitive to its bulk composition.

Combinatorial Methods for Computing Phase Diagram Projections

Combinatorial methods make use of the fact that although there are an infinite number of $P-T-X$ conditions in a phase diagram there are only a finite number of phase equilibria,or phase fields. Consider the system of Fig 1.9a, there are a total of four phases possible in the system, thus there are a total of four one-phase and six two-phase equilibria. The composition of the phases in the two-phase equilibria are fixed, so the phase diagram can be determined in a three step process, first a two-phase assemblage is chosen, say **a**+**c**, then equilibrium composition of **a** and **c** is determined (i.e., the plane tangent to the $\overline{G}-X$ surface of both **a** and **c** is located), and lastly the stability of **a**+**c** is evaluated by testing whether any phases lie below the **a**+**c** $\overline{G}-X$ plane (in Fig 1.9a **a**+**c** is metastable with respect to phases **b** and **d**). If this were repeated for all the two-phase assemblages then all the two-phase fields of the composition diagram would be known, and the identity of the one-phase fields that fill the gaps between the two-phase fields could be determined from the two-phase fields. Strategies of this sort are used in a number of metallurgical programs, they become a little more complicated for multicomponent systems, but they are generally quite efficient and reliable (e.g., Sundman et al. 1985, Lukas et al. 1982).

Schreinemakers Projections, GEO-CALC and THERMOCALC

For phase diagrams as a function of $P-T$ combinatorial methods become less efficient because *c*-phase assemblages are stable over regions in $P-T$ space, and these regions can only be determined by incremental or grid mapping. However, the combinatorial method is still feasible for the calculation of Schreinemakers projections, because in this case it is only necessary to determine the stability of *c*+1-phase assemblages. A simple combinatorial method algorithm for this is: (i) a *c*+1 phase assemblage is selected, (ii) temperature (or pressure) is specified, (iii) the equilibrium pressure and the equilibrium compositions of the phases are determined (i.e., the $\overline{G}-X$ plane), and (iv) the stability of the equilibrium is tested. The temperature is then incremented and steps (ii)-(iv) repeated until the stability of equilibrium has been determined over the entire temperature range of the diagram (Fig 1.10b). This process is repeated for every possible permutation of *c*+1 phases. This method was implemented by Perkins et al. (1986) in a computer program now called GEO-CALC for calculating Schreinemakers projections as a function of $P-T-X^{\mathbf{f}}_{\mathrm{CO2}}$.

In the computer program THERMOCALC, Powell & Holland (1990) have used a similar but more efficient strategy. Neither THERMOCALC nor GEO-CALC are capable of treating solution phases in a fully automated mode (all the programs are capable of making activity corrections; however, fixed activity corrections are almost always thermodynamically inconsistent and should be avoided, as discussed earlier), but THERMOCALC can be used to calculate solution phase equilibria (although it will not tell you if they are stable).

A drawback of combinatorial methods is that they become inefficient as the number components and possible phases for a system, because the number of *c*+1-phase permutations rapidly becomes large. For example in the system CaO-SiO_2-Al_2O_3-CO_2-H_2O there are a total of about 80 phases possible and the number of *c*+1 phase permutations is 3.2×10^8, each of which must be tested for stability.

Solution Phase Equilibria with THERMOCALC and the "Gibbs Method"

The most popular methods of treating metamorphic phase equilibria involving solutions make use of phase equilibrium calculators (Powell & Holland, 1988; Powell et al., 1988; Spear 1988; see also Hillert, 1981). The strategy of Powell et al. (1998) as implemented in THERMOCALC is distinguished from free-energy minimization in that the phases of an equilibrium are specified, rather than the variables of the system. THERMOCALC computes the equilibrium compositions of the coexisting phases, but, in contrast to a minimization

technique, does not test the stability of the assemblage. The calculator can also determine whether the assemblage is possible for a specified bulk composition of a system, and if it is, the environmental conditions at which one phase in the equilibrium vanishes. These conditions may define a phase field boundary in a phase diagram section. Because phase field boundaries can be located directly, rather than by the iterative procedures, the technique offers some advantages over free-energy minimization. Spear (1988) advocates a strategy by which the changes in the phases of a stable equilibrium are determined as a function of environmental variables by application of the Gibbs-Duhem relation in conjunction with mass balance constraints, i.e., the "Gibbs Method". This technique permits a user to model the evolution of a system as a function of its environmental variables from an initial condition that is assumed to be a stable equilibrium. As with Holland and Powell's strategy, this methodology can be used to determine the conditions when a phase disappears from a system due to homogeneous equilibration in response to changing environmental conditions. Because these techniques do not directly establish the stability of equilibria, construction of a phase diagram section by these methods is labor intensive and requires a priori knowledge of phase stabilities.

Perple_X

The necessity for combinatorial methods arises from the difficulties involved in evaluating and keeping track of all the changes that occur on the minimum $\overline{G}$ surface of a system as a function of *P* and *T*. These difficulties have been overcome by a simple linear algorithm for evaluating thermodynamic surfaces (Connolly & Kerrick, 1987) used in the Perple_X program (Connolly 1990). Through this algorithm it is possible to calculate composition diagrams, i.e. chemographies, for systems with an unlimted number of components. It is then a relatively simple matter to monitor the changes in such chemographies as a function of variables like pressure and temperature in order to obtain mixed-variable phase diagrams or Schreinemakers-type phase diagram projections. The advantages of this method are twofold; it can be used to calculate any kind of phase diagram; and, in contrast to pure combinatorial methods, it is extremely efficient and virtually independent of the number of phases considered in a calculation. In addition the program can be used to treat highly non-ideal solutions.

The Perple_X algorithm is numerically exact only for phases with fixed composition. For problems in which it is necessary to consider phases of variable composition, Perple_X approximates the continuous $\overline{G} - X$ surface of solutions by a series of arbitrarily defined compounds, designated pseudocompounds. As a result, the $\overline{G} - X$ surface of each phase is

approximated as a polyhedron, the vertices of which are the pseudocompounds (Fig 1.11). The user controls the number and positions of the pseudocompounds, and thereby the accuracy of the approximation. The primary weakness of the pseudocompound approximation is that it becomes impractical for solutions with more than seven species mixing on a single lattice site.

Problems

1) The Gibbs energy (J/mole of phase) of Quartz (SiO_2), Forsterite (Mg_2SiO_4), Enstatite ($MgSiO_3$), and Periclase (MgO) are -856287.6, -2055023.0, -1458181.0, and -569209.3, respectively (at 298.15 K and 1 bar). Use these data to construct a $\overline{G} - X$ diagram for the system MgO-SiO_2. What are the stable assemblages? What is the μ_{SiO2} for the assemblage forsterite+enstatite? Be careful to distinguish between the free energy per mole of phase and the free energy per mole of system components ($\overline{G}$).
2) What would the isobaric *T–X* diagram look like if β first became tangent to the α+γ $\overline{G} - X$ plane to the left of α in Fig 1.7.
3) The $\overline{G} - X$ surfaces of ordered solution phases tend to have strong curvatures, whereas disordered phases tend to have relatively flatter $\overline{G} - X$ surfaces. Based on this, draw an isobaric *T–X* diagram showing the transition from an ordered to disordered binary solution.
4) If the upper thermal stability of a ternary garnet is limited by a eutectoidal reaction, how many univariant curves will appear limiting the upper thermal stability of garnet in a Schreinemakers projection?

Annotated Bibliography

Berman, R. G., 1988. Internally consistent thermodynamic data for minerals in the system Na_2O-K_2O-CaO-MgO-FeO-Fe_2O_3-SiO_2-TiO_2-H_2O-CO_2. *Journal of Petrology*, **29**, 445-552. Thermodynamic data for minerals derived by linear programming, see Berman & Aranovich (1996).

Berman, R. G. & Aranovich, L. Y., 1996. Optimized standard state and solution properties of minerals. I. Model calibration for olivine, orthopyroxene, cordierite, garnet and ilmenite in the system FeO-MgO-CaO-Al_2O_3-TiO_2-SiO_2. *Contributions to Mineralogy and Petrology*, **126**, 1-24. Thermodynamic data for minerals derived by linear programming, good quality for most phases with high fidelity to the experimental data sources. Essentially a revision of the Berman (1988) data base.

Berman, R. G., Brown, T. H. & Perkins, E., 1987. GEO-CALC: Software for calculation and display of pressure-temperature-composition phase diagrams. *American Mineralogist*, **72**, 861-862. A brief description of the Perkins et al. (1986) programs; the title is misleading, the programs compute P-T-XCO_2 phase diagram projections. Only generally available for IBM-PC computers.

Connolly, J. A. D., 1990. Multivariable phase diagrams: an algorithm based on generalized thermodynamics. *American Journal of Science*, **290**, 666-718. An almost unintelligible description of the Perple_X diagram algorithm (outdated) and some generalized thermodynamics.

Connolly, J. A. D. & Kerrick, D. M., 1987. An algorithm and computer program for calculating composition diagrams. *CALPHAD*, **11**, 1-54. A description of the essential algorithm in Perple_X; outdated, but comprehensible.

Connolly, J. A. D. & Petrini, K., 2000. An automated strategy for calculation of phase diagram sections and retrieval of rock properties as a function of physical conditions. *Journal of Meamorphic Petrology*, **In press**. A description of the current Perple_X algorithm and its application to phase diagram sections.

DeCapitani, C. & Brown, T. H., 1987. The computation of chemical equilibria in complex systems containing non-idel solutions. *Geochimica Cosmochimica Acta*, **51**, 2639-2652. A general free energy minimization program, includes programs for the construction of phase diagram sections, uses UBC mineral data (e.g., Berman, 1988; Berman & Aranovich, 1996).

Eriksson, G. & Hack, K., 1990. Chemsage - a computer program for the calculation of complex chemical equilibria. *Metallurgical Transactions B*, **21B**, 1013-1023. An update on the most widely used free energy minimization program.

Harvie, C. E., Greenberg, J. P. & Weare, J. H., 1987. A chemical equilibrium algorithm for highly non-ideal systems: Free energy minimization. *Geochimica Cosmochimica Acta*, **51**, 1045-1057. A general minimization algorithm that has sucessfully been applied to melt and aqueous systems.

Helgeson, H. C., Delany, J. M., Nesbitt, H. W. & Bird, D. K., 1978. Summary and critique of the thermodynamic properties of rock forming minerals. *American Journal of Science*, **278-A**, 1-229. The first widely used geological thermodynamic data base. The data base has been updated (SUPCRT92) and includes many data for aqueous problems a copy can be obtained from the Laboratory of Theoretical Chemistry at Berkely.

Hillert, M., 1981. A discussion of methods for calculating phase diagrams. *Bulletin of Alloy Phase Diagrams*, **2**, 265-268. Description of an elegant combinatorial phase diagram algorithm.

Hillert, M., 1985. A review of phase diagram principles. *International Metallurgical Reviews*, **30**, 45-65. My favorite review of phase diagrams principles, presented in a general form.

Holland, T. J. B. H. & Powell, R., 1998. An internally consistent thermodynamic data set for phases of petrological interest. *Journal of Metamorphic Geology*, **16**, 309-343. The broadest thermodynamic data base for minerals. Derived by regression analysis. The latest update should be obtained from Holland, the paper also presents some examples of the use of THERMOCALC and describes how to obtain the program.

Korzhinskii, D. S., 1959. *Physicochemical basis of the analysis of the paragenesis of minerals*. Consultants Bureau, Inc., New York. A classic text on phase petrology.

Lukas, H. L., Weiss, J. & Henig, E.-T., 1982. Strategies for the calculation of phase diagrams. *CALPHAD*, **6**, 229-251. A description of free energy minimization techniques coupled with strategies for phase diagram calculation.

Palatnik, L. S. & Landau, A. I., 1964. *Phase equilibria in multicomponent systems*. Holt, Rinehart, and Winston, Inc., New York. A good introduction to thermodynamics and phase diagrams.

Perkins, E. H., Brown, T. H. & Berman, R. G., 1986. PTX-SYSTEM: Three programs for calculation of pressure-temperature-composition phase diagrams. *Computers and Geosciences*, **12**, 749-755. A brief description of Perkin's combinatorial phase diagram projection program, this program is the basis of both GEOCALC and TWEEQU. The title is misleading, the programs compute P-T-XCO_2 phase diagram projections. Although Berman et al. (1987) do not provide the source code of this program, it is possible to get the source code from Perkins, and therefore to compile the programs for computers other than IBM PC's.

Powell, R. & Holland, T. J. B. H., 1988. An internally consistent thermodynamic dataset with uncertainties and correlations: 3. application to geobarometry worked examples and a computer program. *Journal of Metamorphic Geology*, **6**, 173-204.

Powell, R., Holland, T. J. B. H. & Worley, B., 1998. Calculating phase diagrams involving solid solutions via non-linear equations, with examples using THERMOCALC. *Journal of Metamorphic Geology*, **16**, 577-588. A tutorial on the use of solution models for THERMOCALC.

Saxena, S. K. & Eriksson, G., 1983. Theoretical computation of mineral assemblages in pyrolite and lherzolite. *Journal of Petrology*, **24**, 538-555. An example of the application of Eriksson's minimization program SOLGASMIX for calculating phase diagram sections.

Spear, F. S., 1988. The Gibbs method and Duhem's theorem: The quantitative relationships among P, T, chemical potential, phase composition and reaction progress in igneous and metamorphic systems. *Contributions to Mineralogy and Petrology*, **99**, 249-256. A comprehensive description of the "Gibbs Method" algorithm. This algorithm has been

programmed and can be used to calculate the variation in an equilibrium assemblage from an assumed initial condition. A popular tool for thermobarometry. The program and extensive documentation can be obtained from Spear.

Sundman, B., Jansson, B., & Andersson, J.-O., 1985. Thermo-Calc databank system. *CALPHAD*, **9**, 153-186. This is not the petrological THERMOCALC of Powell and Holland, but rather a sophisticated program for calculating alloy phase diagrams, the program is entirely general and could be of value for petrologic problems.

Van Zeggeren, F. & Storey, S. H., 1970. *The computation of chemical equilibria*. Cambridge University Press, Cambridge. A discussion of minimization techniques.

Wood, B. J. & Holloway, J. R., 1984. A thermodynamic model for subsolidus equilibria in the system CaO-MgO-Al_2O_3-SiO_2. *Geochimica Cosmochimica Acta*, **66**, 159-176. Application of a minimization program for calculation of constant composition phase diagram sections, the program is available, but it is not very flexible.

Zen, E.-A., 1966. Construction of pressure-temperature diagrams after the method of Schreinemakers--A geometric approach. In: *U. S. Geological Survey Bulletin*, pp. 56. An introduction to Schreinemakers projections.

Figure Captions

Fig 1.1 **a**) $\overline{G} - X$ diagram for an isobaric-isothermal binary system illustrating equilibration in terms of the minimum energy criterion (Eq 1.1). If the system initially consists of parts a and b, its molar Gibbs energy is given by the value where the line connecting a and b coincides systems composition. The system can lower its energy if the composition of a and b shift toward a' and b'. The system is stable when the compositions of both parts become identical to the bulk composition of the system. **b**) $\overline{G} - X$ diagram for a partially miscible solution. Any composition between a' and b' is metastable with respect to a mixture of a' and b', these compositions define the solutions solvus. Feldspar and micas show this kind of behavior. **c**) $\overline{G} - X$ diagram for a completely immiscible solution. No intermediate solution compositions are stable because the second derivative of free energy with respect to composition is negative for all compositions. For any non-degenerate composition of the system, the stable state is a mixture of phases a' and b', quartz and corundum approximate such a mixture.

Fig 1.2 **a**) A system is in internal equilibrium when no thermodynamic processes are possible among the existing phases of the system, i.e., when the potential for any process is uniform throughout the system. **b**) Phases a and b cannot be in equilibrium because the chemical potentials are not equal in both phases. **c**) A spontaneous process may occur in a system initially in internal equilibrium, in an isolated system such processes occur so as to increase the entropy of the system, in an isobaric-isothermal system spontaneous processes lower the Gibbs energy of the system.

Fig 1.3 **a**) An isothermal system consisting of the mineral biotite, a solution between the Mg and Fe endmembers phlogopite and annite. The system is connected to two compartments by rigid osmotic membranes that are permeable with respect to only one endmember. At equilibrium the pressure in each compartment is dicatated by the constraint that the partial molar $\overline{G}$ of the pure endmember in the compartment must be equal to that of the endmember in biotite solution. It follows that only one of the three pressures is independent for an equilibrium system. **b**) The conventional definition of the activity of a solution endmember is related to the difference in the partial molar $\overline{G}$ of the endmember in the solution and in its pure state at the same pressure and temperature. Alternatively, activities may be defined relative to the partial molar $\overline{G}$ of the pure endmember at a different pressure, in which case the activity is usually referred to as a fugacity.

Fig 1.4 **a**) The stable states of a heterogeneous system can be determined conceptually by draping a rope under the $\overline{G} - X$ surfaces of the phases and then pulling upwards on the ends of the rope. **b**) When the rope is taut it defines the system minimum $\overline{G}$ surface. This surface is linear where $p=c=2$ phases coexist. In such a region the chemical potentials and phase compositions are determined by the point at which the systems minimum $\overline{G}$ surface is tangent to the surfaces of the coexisting phases and the amounts of the phases are determined by the lever rule. In non-linear regions (i.e., $p<c$ phases) the curvature of the systems minimum $\overline{G}$ surface is always positive, this requires that chemical potentials are proportional to their conjugate compositional variables. **c**) In a system consisting only of compounds, all phase regions consist of $p=c=2$ phases, in the pathological case that the system has exactly the composition of a stable compound the system must be treated as a one-component system because such a compound does not define the chemical potentials of the components in the two-component system.

Fig 1.5 **a**) $\overline{G} - X$ diagrams illustrating that the compositions of coexisting phases in a divariant equilibrium are a unique function of pressure and temperature and therefore a potential thermobarometer, higher variance assemblages may also serve this purpose, but their compositions depend also on the composition of the system. **b**) In conventional thermobarometry measured phase compositions are assumed to be those of a relict equilibrium, the conditions of an activity-corrected equilibrium based on these compositions are the conditions at which the partial molar $\overline{G}$ of the endmembers are equal in a subcomposition of the system. **c**) *P*–*T* conditions of the activity-corrected phl=py and ann=alm "univariant" equilibria, and the true univariant equilibrium of biotite with staurolite and garnet. **d**, **e**, and **f**) $\overline{G} - X$ diagrams corresponding to various points in **c**.

Fig 1.6 A composition phase diagram is the projection of the stable phase relations of a systems minimum $\overline{G}$ surface onto composition space. Alternatively, a second phase diagram which shows the phase relations of the system as a function of the μ_1 can be derived from the projection of the tangent of the systems minimum $\overline{G}$ surface.

Fig 1.7 The relation between an isobaric *T*–*X* mixed variable diagram and $\overline{G} - X$ diagrams. Since the $\overline{G} - X$ diagrams depend also on pressure, it is to be expected that all the features of the *T*–*X* diagram, such as the eutectic reaction stoichiometry, will depend on pressure as well.

Fig 1.8 **a**) The simplest possible multicomponent phase diagram is three-dimensional; such diagrams may be simplified by either sectioning (**b**) or projection (**c** and **d**). None of these simplifications are proper phase diagrams because they do not completely define the state of the system and its constituent phases. Projections may be complicated by singular equilibria that limit special phase compositions, in general there must be at least two singular equilibria for every eutectoidal equilibrium as illustrated in **f**.

Fig 1.9 **a**) Classical minimization strategies involve two major components, one component is to establish the equilibrium of phase assemblage such as a+c, the second component determines whether this equilibrium is stable. **b**) A virtue of minimization strategies is that the user is completely free to specify any point or path through the systems multidimensional parameteric space. **c**) Minimization can be used to construct a phase diagram or phase diagram section by computing stable assemblages on a grid defined by the variables of interest; however, the phase boundaries must be determined by interpolation between the grid points.

Fig 1.10 In combinatorial strategies phase assemblages are enumerated and their stability is tested, these strategies are only feasible for systems in which all phases are compounds (or activity-corrected compounds). The PTX program, and its numerous derivatives, strategy involves enumeration of univariant assemblages, THERMOCALC differs in that divariant assemblages are enumerated. Neither of these strategies define the higher variance equilibria of a system and therefore cannot be used to construct true phase diagrams. THERMOCALC offers a second computational mode that is capable of computing equilibria involving solutions, but, at present, in this mode the program doesnot test the stability of the equilibria. PERPLE_X determines all phase equilibria, irrespective of variance, and therefore can be used to construct any kind of phase diagram. In PERPLE_X solutions are modeled by approximating solution behavior by a series of discrete compounds referred to as "pseudocompounds".

Fig 1.11. In the pseudocompound approximation, pseudocompounds are used to define the possible compositions of solutions, e.g., the solution B is represented by pseudocompounds $B_1 \ldots B_8$, the accuracy of this representation is determined by the

pseudocompound spacing. PERPLE_X determines which of the pseudocompounds are stable and thereby the approximate stability field of the corresponding solution. Given current computational resources, such calculations can be made with essentially unlimited accuracy.

Fig 1.12 A composition phase diagram computed with PERPLE_X for the CaO-SiO_2-Al_2O_3 at super-solidus conditions. The melt field (shaded) is divided into triangular regions defined by the stable pseudocompounds used to represent the melt phase.

Fig 1.13 A mixed variable phase diagram computed with PERPLE_X. The stepped phase boundaries are due to the pseudocompound approximation.

Fig 1.14 A phase diagram projection computed with PERPLE_X, the dashed curves correspond to the steps in a mixed variable phase diagram such as illustrated in Fig 1.13. These curves are essentially isoplethal contours of high variance phase fields. Heavy solid curves represent true univariant phase fields.

Fig. 1.1

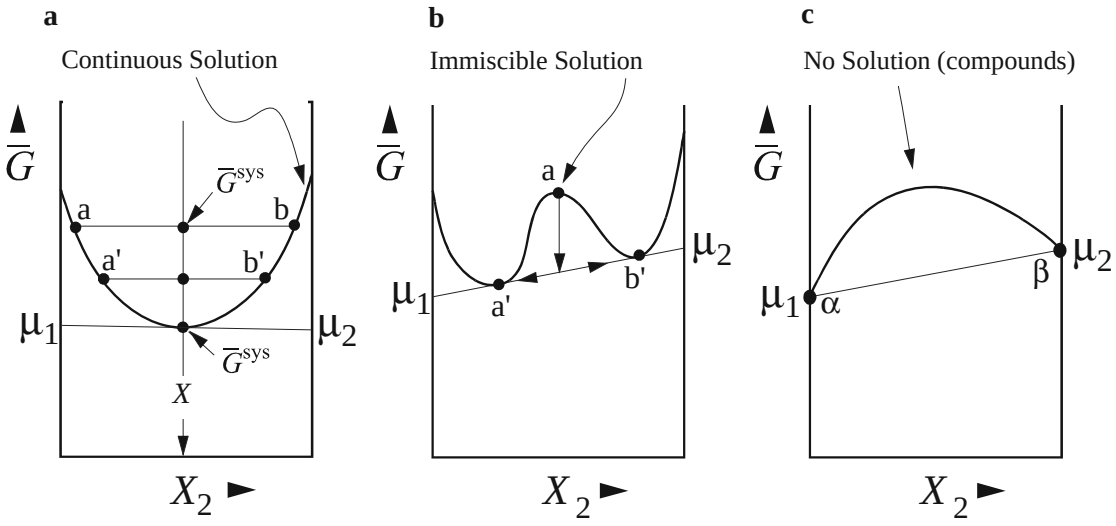
a
Continuous Solution
b
Immiscible Solution
c
No Solution (compounds)
$\overline{G}$
$\overline{G}^{sys}$
a
b
a'
b'
μ_1
μ_2
X
X_2
α
β

Fig. 1.2

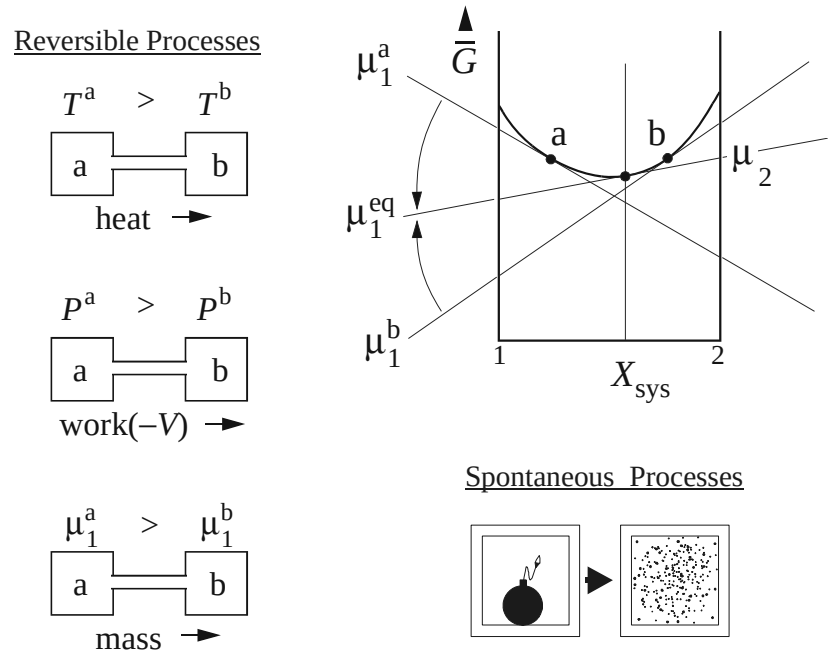
Reversible Processes
$T^a > T^b$
a
b
heat
$P^a > P^b$
work(−V)
$\mu_1^a > \mu_1^b$
mass
$\overline{G}$
μ_1^a
μ_1^{eq}
μ_1^b
μ_2
1
2
X_{sys}
Spontaneous Processes

Fig. 1.3

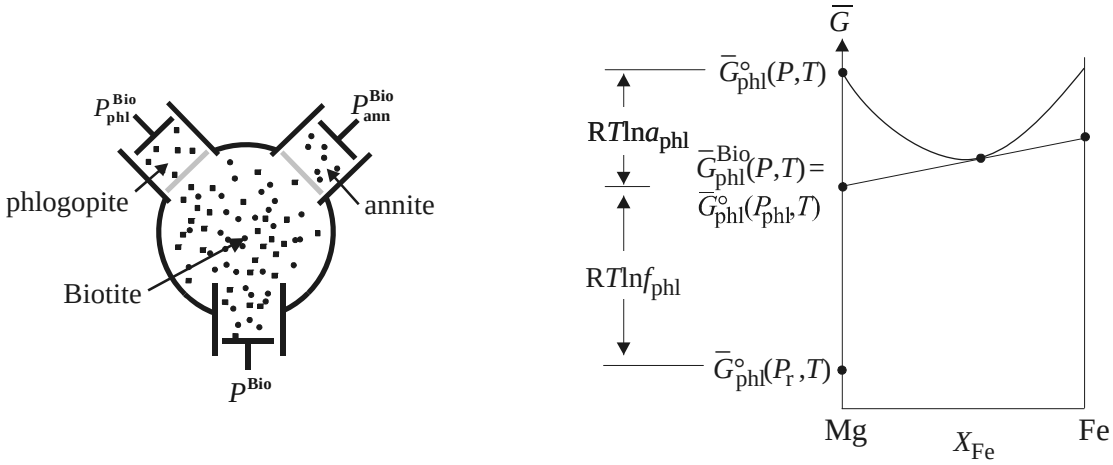
P_{phl}^{Bio}
P_{ann}^{Bio}
phlogopite
annite
Biotite
P^{Bio}
$\overline{G}$
$\overline{G}^{\circ}_{phl}(P,T)$
$RT\ln a_{phl}$
$\overline{G}^{Bio}_{phl}(P,T) =$
$\overline{G}^{\circ}_{phl}(P_{phl},T)$
$RT\ln f_{phl}$
$\overline{G}^{\circ}_{phl}(P_r,T)$
Mg
X_{Fe}
Fe

Fig. 1.4

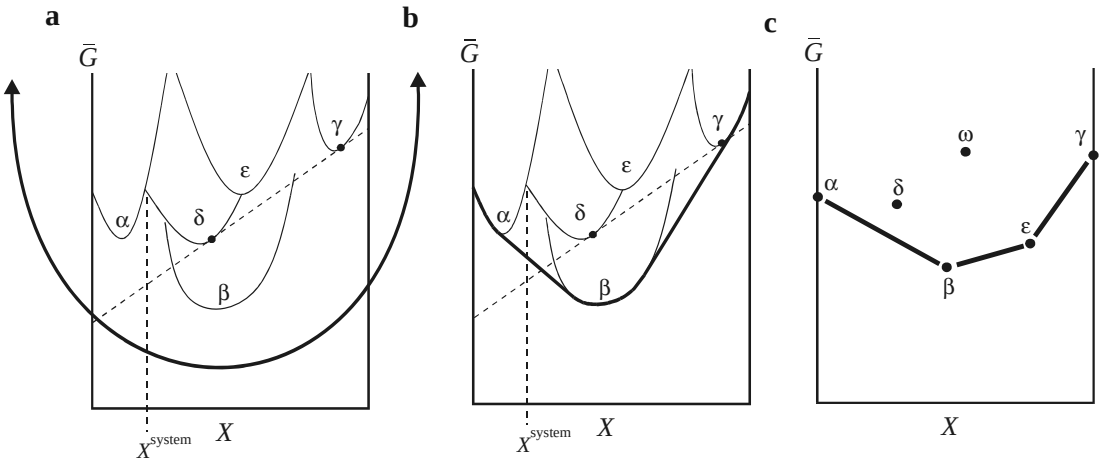
a
b
c
$\overline{G}$
α
β
γ
δ
ε
ω
X^{system}
X

Fig. 1.5

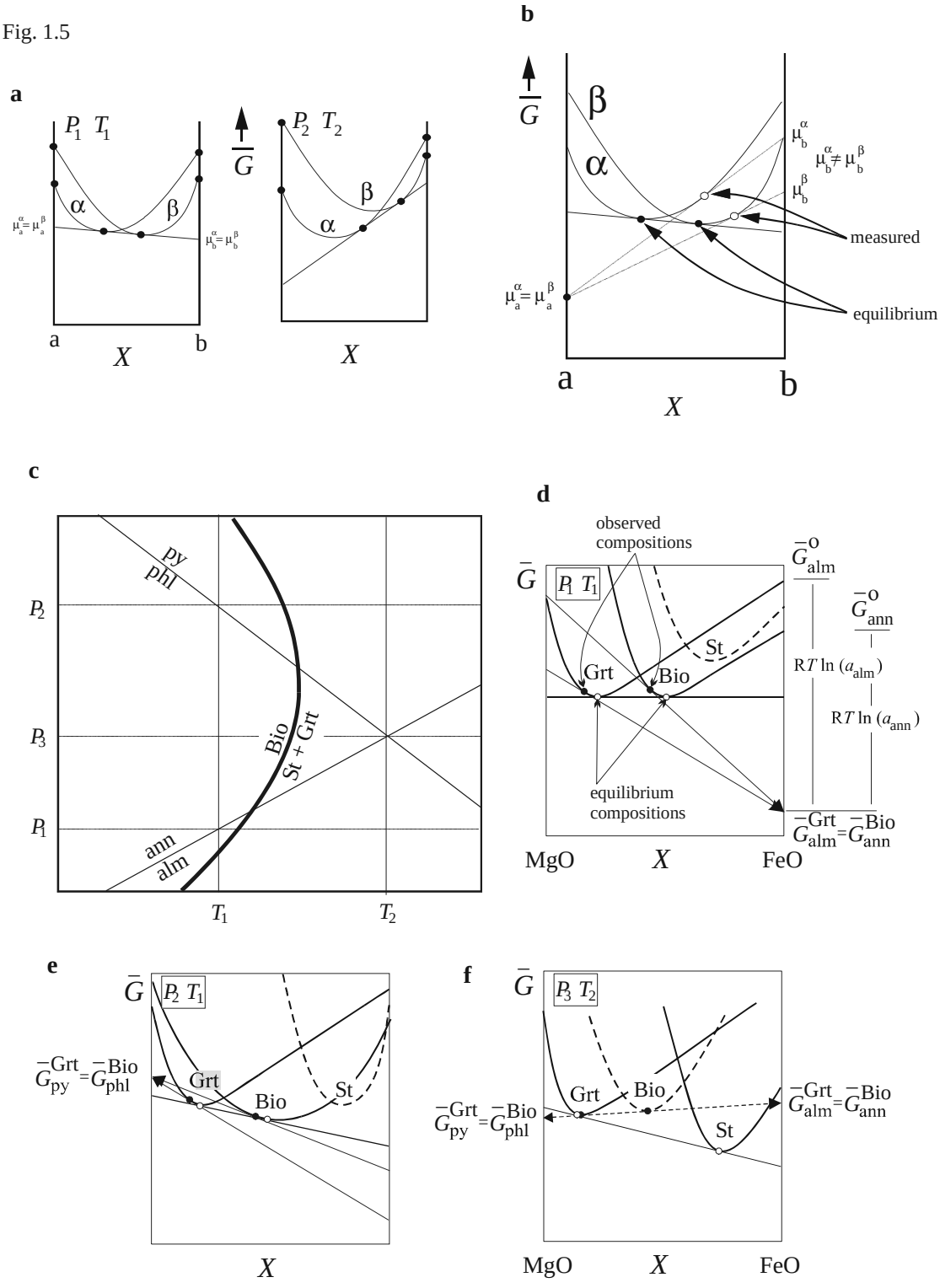
a
P1 T1
α
β
G
P2 T2
β
α
a
X
b
X
b
G
β
α
measured
equilibrium
a
X
b
c
py
phl
P2
P3
P1
Bio
St + Grt
ann
alm
T1
T2
d
observed
compositions
G
P1 T1
St
Grt
Bio
equilibrium
compositions
RT ln (aalm)
RT ln (aann)
MgO
X
FeO
e
G
P2 T1
Grt
Bio
St
X
f
G
P3 T2
Grt
Bio
St
MgO
X
FeO

Fig. 1.6

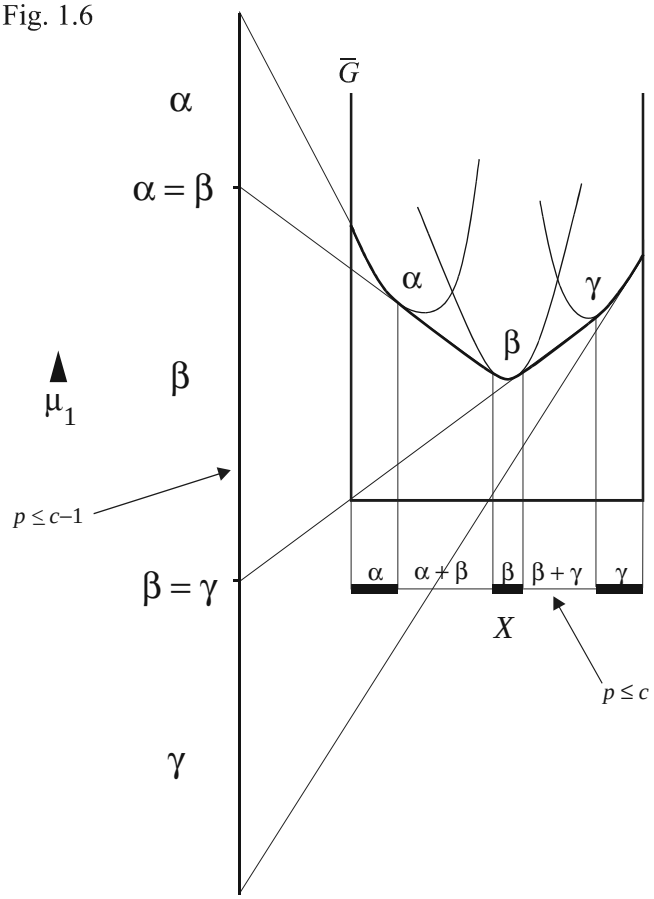

Fig. 1.7

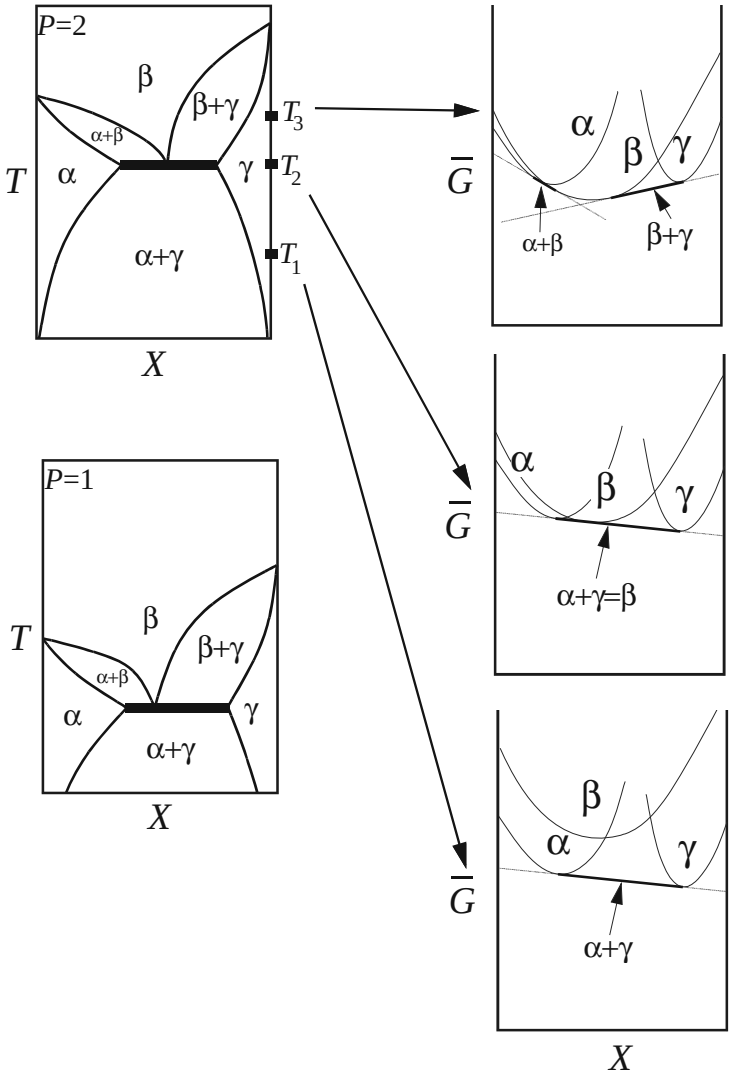

Fig. 1.8

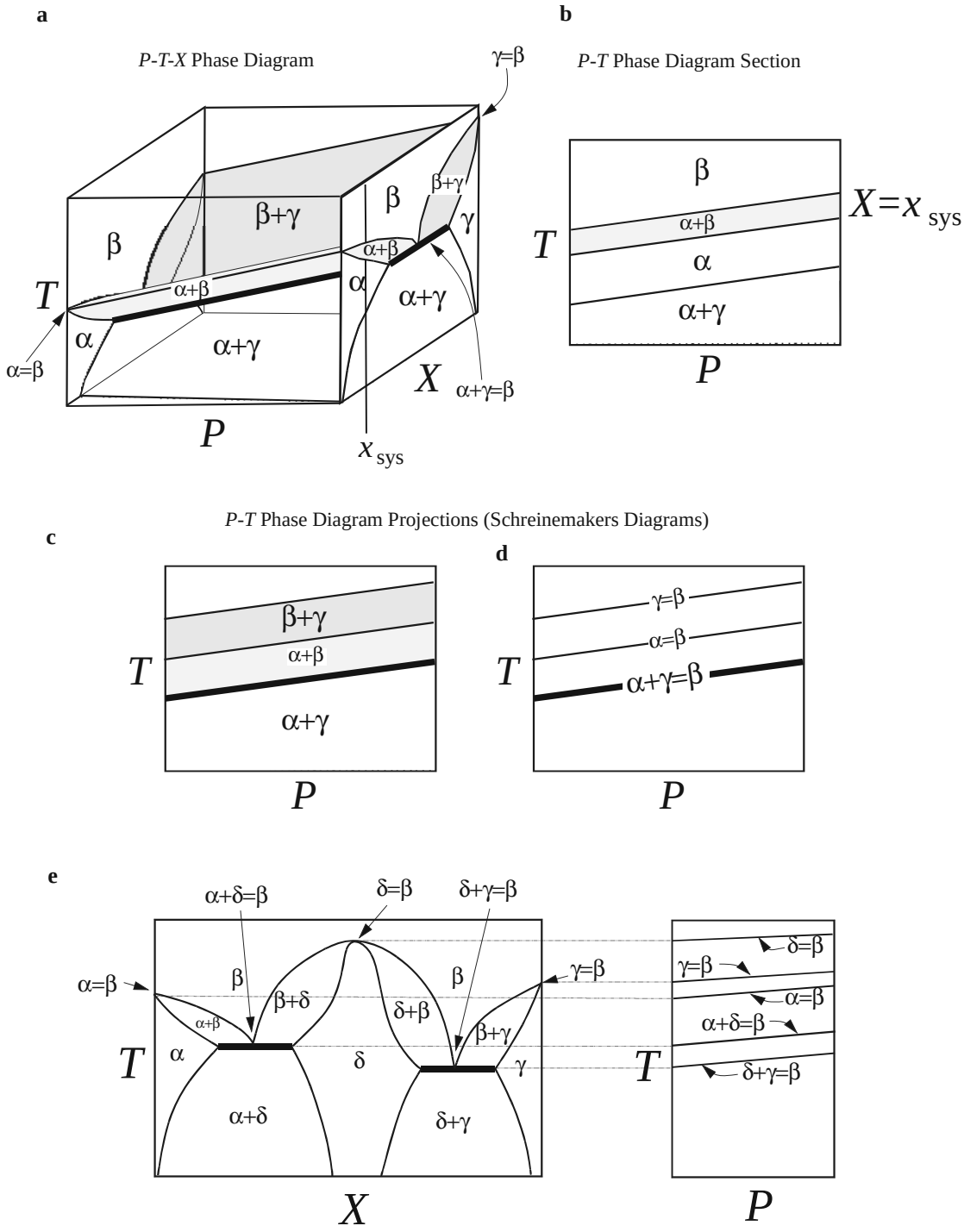
a
P-T-X Phase Diagram
γ=β
β
β+γ
β
β+γ
γ
α+β
α+β
α
α+γ
T
α
α+γ
α=β
X
α+γ=β
P
x sys
b
P-T Phase Diagram Section
β
X=x sys
α+β
T
α
α+γ
P
P-T Phase Diagram Projections (Schreinemakers Diagrams)
c
β+γ
α+β
T
α+γ
P
d
γ=β
α=β
T
α+γ=β
P
e
α+δ=β
δ=β
δ+γ=β
α=β
β
β+δ
δ+β
β
β+γ
γ=β
α+β
T
α
δ
γ
T
α+δ
δ+γ
X
δ=β
γ=β
α=β
α+δ=β
δ+γ=β
P

Fig. 1.9

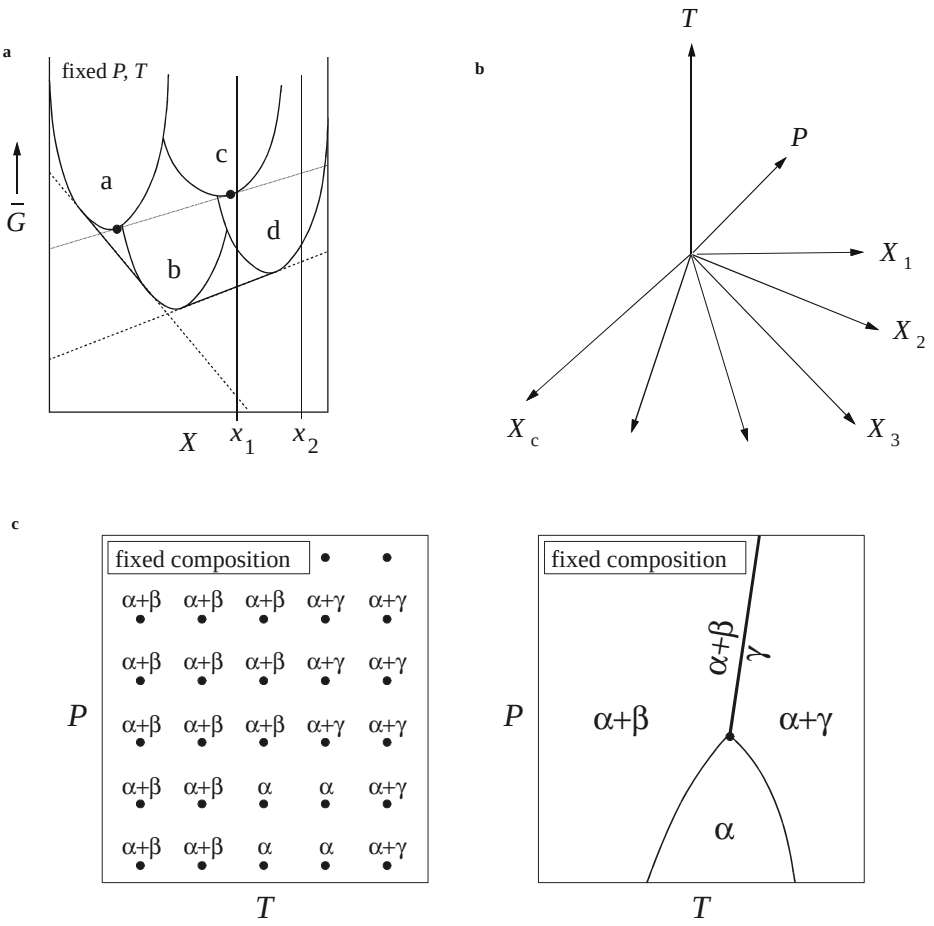
a
fixed P, T
G
a
b
c
d
X
x1
x2
b
T
P
X1
X2
X3
Xc
c
fixed composition
α+β
α+γ
α
P
T
fixed composition
α+β
γ
α+β
α+γ
α
P
T

Fig. 1.10

Combinatorial Phase Diagram Projection Methods

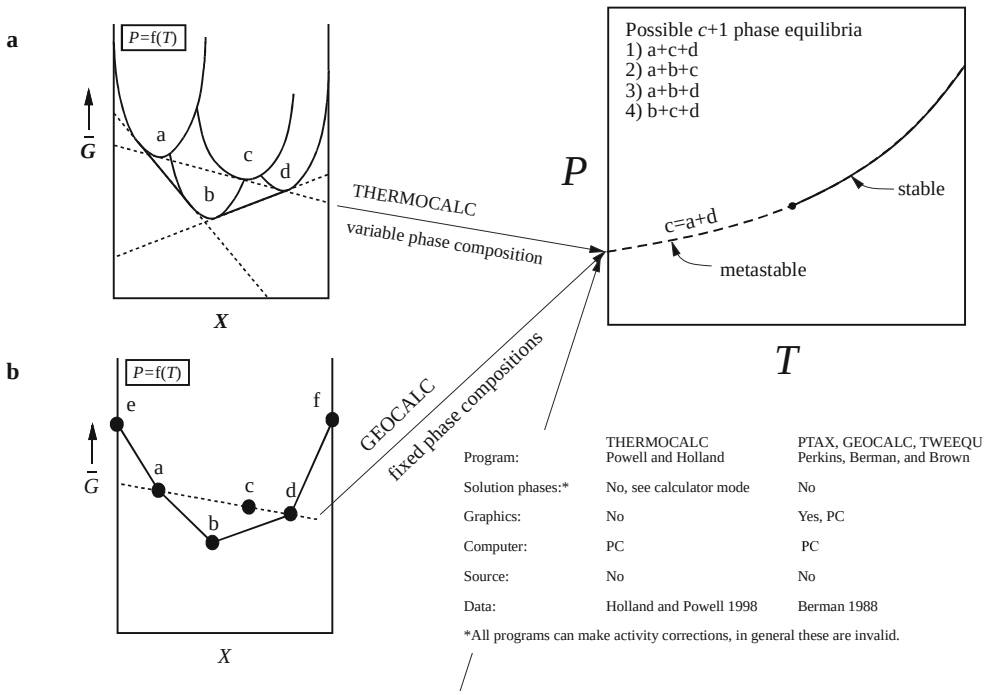

Program:	THERMOCALC Powell and Holland	PTAX, GEOCALC, TWEEQU Perkins, Berman, and Brown
Solution phases:*	No, see calculator mode	No
Graphics:	No	Yes, PC
Computer:	PC	PC
Source:	No	No
Data:	Holland and Powell 1998	Berman 1988

*All programs can make activity corrections, in general these are invalid.

Non-combinatorial Phase Diagram Calculation

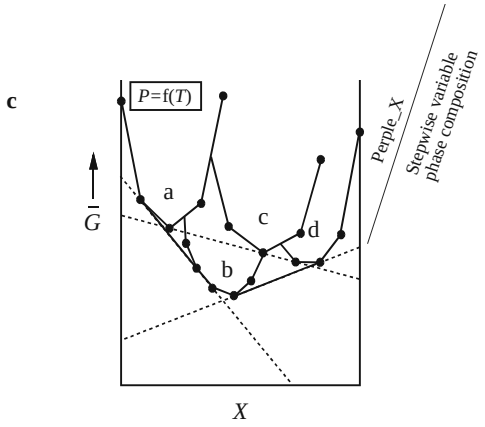

There are no restrictions
on the solution models, computers,
or data sources used for Perple_X

Figure 1.11

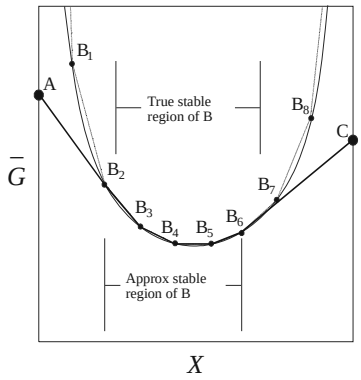

Figure 1.12

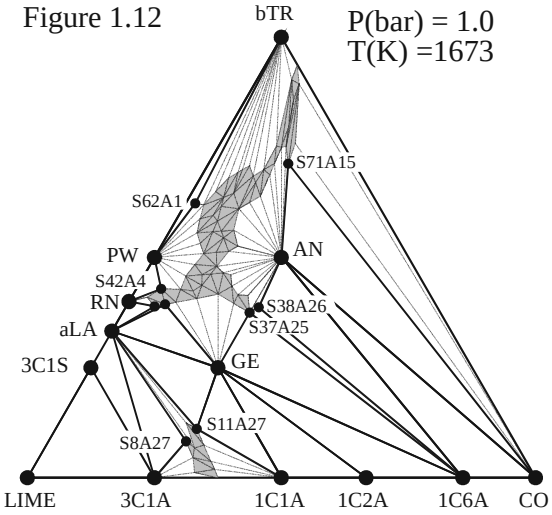

Figure 1.13

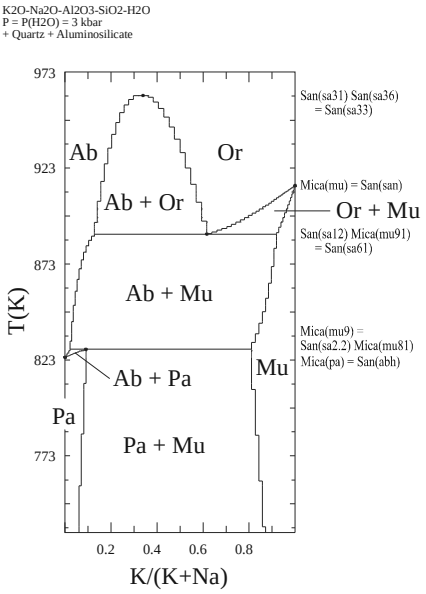

Figure 1.14